

Observation of a Structural Transition for Coulomb Crystals in a Linear Paul Trap

Niels Kjærgaard*

Optics and Fluid Dynamics Department, Risø National Laboratory, DK-4000 Roskilde, Denmark

Michael Drewsen†

QUANTOP—Danish National Research Center for Quantum Optics, Department of Physics and Astronomy, University of Aarhus, DK-8000 Aarhus C, Denmark

(Received 21 March 2003; published 27 August 2003)

A structural transition for laser cooled ion Coulomb crystals in a linear Paul trap just above the stability limit of parametrically resonant excitation of bulk plasma modes has been observed. In contrast to the usual spheroidal shell structures present below the stability limit, the ions arrange in a “string-of-disks” configuration. The spheroidal envelopes of the string-of-disks structures are in agreement with results from cold fluid theory usually valid for ion Coulomb crystals if the ion systems are assumed to be rotating collectively.

DOI: 10.1103/PhysRevLett.91.095002

PACS numbers: 52.27.Lw, 52.27.Jt

When non-neutral ion plasmas confined by external electromagnetic potentials are cooled to temperatures in the millikelvin regime, ordered structures referred to as Coulomb crystals can be formed. By laser cooling atomic ions, Coulomb crystals of various shapes and sizes in effectively harmonic trapping potentials of both Penning and Paul (rf) traps have been studied for more than a decade [1–7]. Moreover, molecular dynamics simulations of the equilibrium state of such cooled, non-neutral plasmas under various realistic trapping conditions have been performed to investigate the structural properties of Coulomb crystals (see [8] and references therein). For example, in the case of cylindrically symmetric harmonic potentials it is known that cold, small crystals (without too extreme aspect ratios) arrange in closed, concentric spheroidal shells [8]. Furthermore, the outer, spheroidal boundary is in excellent agreement with what is found in an analytical charged liquid model—a result which has also been confirmed experimentally for a linear Paul trap [9,10]. In the linear Paul trap, the description of the trapping potential as being effectively harmonic is complicated by the presence of a time-varying quadrupole field. In particular, at high rf powers, where the plasma frequency ω_p exceeds half the rf drive frequency ω_{rf} , a parametric resonance can be excited leading to instability. This was experimentally confirmed in [11], where spheroidal shell Coulomb crystals were observed to transform into a cloud state at this stability limit.

In this Letter, we report the observation of a structural transition of $^{24}\text{Mg}^+$ ion Coulomb crystals in a linear Paul trap. The transition appears at an rf power where the plasma frequency just exceeds half the rf drive. In contrast to the conventional closed-shell structure, the ions arrange in a “string-of-disks” type of configuration. The structural transformation is accompanied by a dramatic and counterintuitive change in the aspect ratio of the outer envelope of the trapped ion plasma.

Figure 1(a) shows a sketch of the linear Paul trap applied in the experiments. In Cartesian coordinates with z taken to be the axial direction of the trap, the total time-varying electric potential of our linear Paul trap is given by

$$\Psi(x, y, z, t) = \frac{U_{rf}(t)}{2r_0^2}(x^2 - y^2) + \frac{U_{dc}\eta}{2z_0^2}[2z^2 - (x^2 + y^2)], \quad (1)$$

where $U_{rf}(t)$ is a periodic rf voltage of amplitude V_{rf} and angular frequency ω_{rf} applied to the quadrupole rods, r_0 is the inscribed radius of the interelectrode space, U_{dc} is the voltage difference between the end pieces and the center pieces of the quadrupole rods, η is a geometric factor for the trap, and z_0 is the length of the electrode

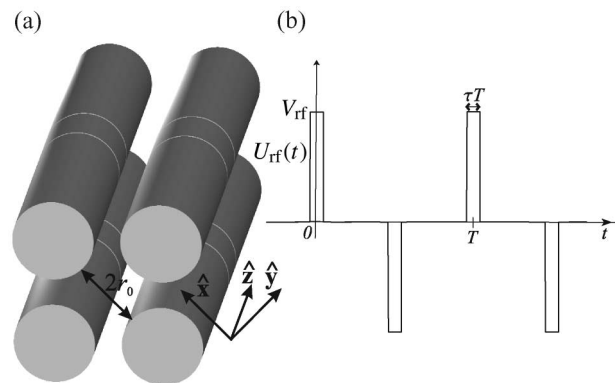


FIG. 1. (a) Sketch of the linear Paul trap. Time-varying voltages are applied to the electrodes so that the resulting voltage difference between adjacent rods is given by $U_{rf}(t)$ leading to radial confinement of ions. To obtain axial confinement, each electrode is sectioned into three and an additional dc voltage U_{dc} is applied to the eight end pieces with respect to the center pieces. (b) The pulsed, time-varying waveform $U_{rf}(t)$.

center pieces. For a particle of charge e and mass m the second term (dc term) of the potential given by Eq. (1) gives rise to harmonic confinement along the z axis with corresponding oscillation frequency $\omega_z = \sqrt{-a\omega_{\text{rf}}^2/2}$, where $a = -4\eta eU_{\text{dc}}/mz_0^2\omega_{\text{rf}}^2$. In the radial direction, the effect of this term is to repel particles from the trap axis with a force linear in the radial position. The radial, defocusing force originating from the dc term is counteracted by the pseudoharmonic radially restoring force from the first term (rf term) of the potential Ψ in Eq. (1). The net effective radial oscillation frequency ω_r can be calculated from a and $q = 2eV_{\text{rf}}/mr_0^2\omega_{\text{rf}}^2$ by evaluating the characteristic exponents for the Floquet's solution to Hill's type of equations found by considering the radial part of the equations of motion in the potential Ψ . In the experiments presented here, evenly spaced, rectangular voltage pulses are applied alternately to diagonal pairs of quadrupole rods resulting in a waveform $U_{\text{rf}}(t)$ as shown in Fig. 1(b). The radial, pseudoharmonic confinement potential for charged particles has cylindrical symmetry and the oscillation frequency $\omega_r(q, a)$ may be found using the matrix method of Courant and Snyder [12] as outlined in [13].

The experimental setup has been described in detail in [11]. In short, the linear Paul trap is operated in a pulse-excited mode [13], using the rf waveform shown in Fig. 1(b) of frequency $\omega_{\text{rf}} = 2\pi \times 700$ kHz. $^{24}\text{Mg}^+$ ions are isotope selectively loaded into the trap by resonantly laser photo-ionizing ^{24}Mg atoms effusing from an oven in the direction of the trap [14]. The $^{24}\text{Mg}^+$ ions captured by the trapping fields are laser cooled by two counter-propagating laser beams along the axial direction of the trap (z axis). The light spontaneously emitted by the trapped ions during the laser cooling cycle is recorded by an intensified digital camera system. The camera is read out at a rate of 5 frames/s and views the plasma along the radial direction $-(\hat{x} + \hat{y})/\sqrt{2}$ [see Fig. 1(a)] through the center of the trap.

Figure 2(a) shows an image of a laser cooled $^{24}\text{Mg}^+$ Coulomb crystal containing approximately 370 ions in our trap. The image was recorded with a trap q parameter just below the point of occurrence of parametric instability for crystals. As expected [8–10], the ions form closed, spheroidal shells and the correspondence between the effective radial-to-axial confinement force ratio

$$\beta \equiv \frac{\omega_r^2}{\omega_z^2} \quad (2)$$

and the spheroidal envelope aspect ratio α ($\alpha \equiv Z/R$, where Z and R are the axial and radial axes, respectively) is well described by the cold fluid relation

$$\beta = \frac{1}{2} \left(\left\{ \frac{1-\gamma^2}{\gamma^2} \left[\frac{1}{1-\gamma^2} - \frac{1}{2\gamma} \ln \left(\frac{1+\gamma}{1-\gamma} \right) \right] \right\}^{-1} - 1 \right)^{-1}, \quad (3)$$

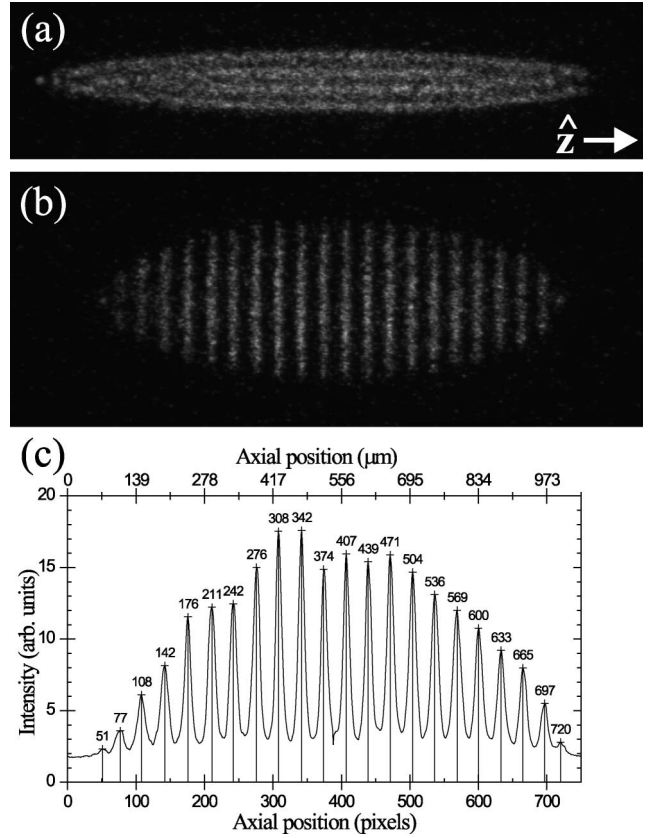


FIG. 2. Laser cooled $^{24}\text{Mg}^+$ plasma containing approximately 370 ions in Coulomb crystal configurations just below (a) and above (b) the $2\omega_p = \omega_{\text{rf}}$ dynamical instability. (c) The integrated axial intensity distribution of the string-of-disks configuration (b) showing the disk locations; the disks are near-equidistantly spaced.

where $\gamma^2 = 1 - \alpha^{-2}$. We note that the density of a low-temperature, non-neutral plasma (cold fluid) in a harmonic trap is given by $n_0 = (\epsilon_0 m/e^2)(\omega_z^2 + 2\omega_r^2)$ and that the plasma frequency is

$$\omega_p = \sqrt{e^2 n_0 / \epsilon_0 m} = \sqrt{\omega_z^2 + 2\omega_r^2}. \quad (4)$$

A surprising observation was made by increasing q [leads to an increase in ω_r and hence ω_p ; cf. Eq. (4)] slightly above the point of occurrence of the parametric resonance $2\omega_p = \omega_{\text{rf}}$. Passing this critical value of q , the plasma transforms from the normal, radially ordered state in Fig. 2(a) through a temporally cloud state into an axially ordered state as shown in Fig. 2(b). The movie sequence [15] shows the dramatic transition. Assuming cylindrical symmetry, this new state appears as a string of approximately equidistantly spaced disks and the structure differs radically from the initial closed-shell state. Both types of states are well described by an overall spheroidal plasma envelope as expected for very cold plasmas [9,16], but, evidently, the density of the string-of-disks structure in Fig. 2(b) is much lower than the

closed-shell structure in Fig. 2(a). This is in contrast to the fact that the radial confinement of the trap has been increased slightly.

To investigate the string-of-disks state further, we performed a series of measurements where a was varied through U_{dc} while the plasma remained in the axially ordered state. In this way we obtained corresponding values of the spheroidal aspect ratio α and the radial-to-axial confinement force ratio β for the radially ordered state. In Fig. 3 we show $\beta(\alpha)$ for the string-of-disks state as calculated from trap parameters using Eq. (2). The series was recorded with an rf waveform duty cycle $\tau = 0.07$ [see Fig. 1(b)]. The results do not exhibit any agreement either with $\beta(\alpha)$ as derived from the theory of cold, stationary fluids presented by Eq. (3) or with the expected shape dependence of a nonrotating gaseous plasma for which $\beta \approx \alpha^2$. Rotating crystals have, however, recently been observed in a linear Paul trap by introducing a torque on an initial stationary crystal [10]. Hence, it appears natural to analyze the present findings under the hypothesis that the ions undergo a collective rotation about the z axis. Such a rotation will lead to an effective radial defocusing force which in the above theoretical treatment is analogous to introducing a new radial a parameter given by $a_{\text{rad,eff}} = a + a_{\text{rot}}$, where a_{rot} is defined so that $\sqrt{-a_{\text{rot}}}\omega_{\text{rf}}/2$ is the common rotation frequency. For the string-of-disks series, Fig. 4 presents the actual a parameter as calculated from trap parameters, the effective, radial $a_{\text{rad,eff}}$ parameter which brings the measured aspect ratio of the crystal structure in agreement with the cold fluid result of Eq. (4), and the derived value of a potential, rotational contribution a_{rot} . As is evident from this figure, the hypothesis that the ions are

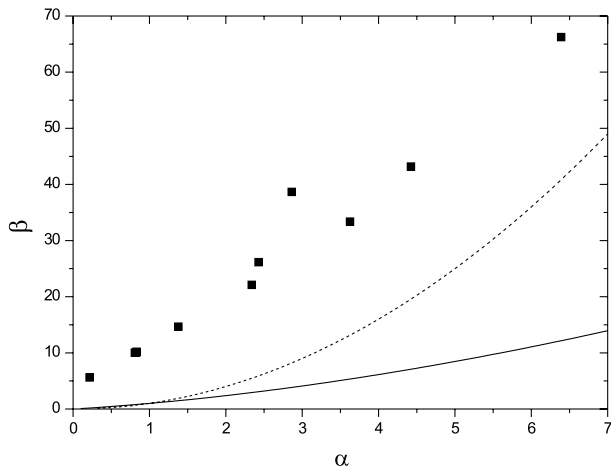


FIG. 3. The correspondence between the aspect ratio α and the radial-to-axial confinement force ratio β for a cold fluid (solid line) and a hot, gaseous plasmas (dashed line). For the string-of-disks state crystal, $\beta(\alpha)$ calculated from experimental trap parameters is about an order of magnitude off both these curves (■).

rotating as a density-limited system at a well-defined frequency of about $\sqrt{0.25}\omega_{\text{rf}}/2 \approx \omega_{\text{rf}}/4$ around the z axis is very plausible. A mechanism leading to rotation is, however, not clear at present, but it could probably be the combined action of a resonant excitation of the bulk plasma mode by some rf multipole mode (e.g., the fundamental quadrupole mode) along with radial momentum diffusion due to the laser cooling process. In any case, the string-of-disks type of state must be closely linked to the rf driving force as the dissipative laser cooling force would otherwise lead to relaxation into a stationary closed-shell structure.

A fact strongly supporting the observed structure to consist of cold disks is the near-equidistant spacing of the axially ordered structures as indicated in Fig. 2(c). Within a few percent, the spacing equals the one expected for 2D hexagonal structures stacked as a 3D hcp structure. Such nearly perfect hcp structures have, indeed, earlier been found in simulations of large infinitely long, cylindrical shell structures [17] and spherical structures [18].

We have observed the string-of-disks state in plasmas of various sizes and, furthermore, by averaging over more frames we have seen a clear indication of ordering within the individual disks (see Fig. 5), albeit this correlation is not as evident as the axial ordering [e.g., in the single-frame crystal image in Fig. 2(b) ordering within disks is not visible]. This might be due to intradisk diffusion of particles similar to the intrashell diffusion known to be present in closed-shell structures [19]. Alternatively, it can be explained by the fact that the radial temperature is

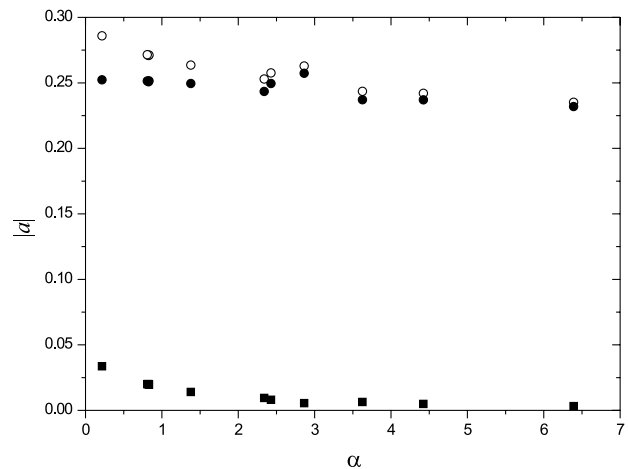


FIG. 4. String-of-disks configuration. The magnitude of the trap a parameter originating from the voltage difference between the end pieces and the center pieces of the quadrupole rods (■) and the magnitude of the effective a parameter necessary to make ω_r sufficiently small for the expressions Eqs. (2) and (3) to be consistent for experiment and cold fluid theory (○). By subtracting the former from the latter we obtain the residual a parameter a_{rot} (●) of fairly constant magnitude ~ 0.25 .

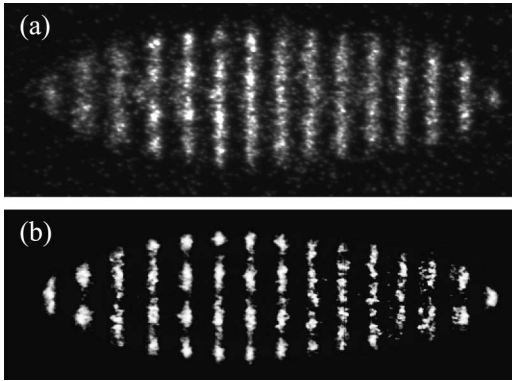


FIG. 5. (a) Single-frame image of a string-of-disks state crystal. (b) By averaging over five frames and enhancing the image contrast, radial ordering becomes visible.

somewhat higher than the axial temperature since the lasers cool only the axial motion directly, whereas the radial motion is cooled sympathetically through Coulomb interactions. The various structural phases of rotating crystallized ion plasmas harmonically confined in a Penning trap have been reported [6], but in none of these experiments was the string-of-disks-type structure shown in Fig. 2(b) observed to appear for prolate crystals (i.e., crystals for which $\alpha > 1$). We have obtained the string-of-disks state using both a pulsed and a sinusoidal voltage excitation of the quadrupole rods, and it seems to constitute a new type of crystal specific to rf traps. There is, at present, no immediate reason for the axial ordering observed in our experiment even if the hypothesis that the crystals are rotating holds. In the previously mentioned experiments [10], where a torque was applied to make crystals rotate below the $2\omega_p = \omega_{rf}$ stability limit, the ions have been observed to remain in the closed spheroidal shells structure.

In conclusion, we have investigated the stability of Coulomb crystals in a pulse-excited linear Paul trap at the $2\omega_p = \omega_{rf}$ stability limit. Just above the stability limit crystals were observed to reappear by rearranging in axially ordered structures, consistent with strings of disks with an overall spheroidal envelope. The observed envelope aspect ratios of the string-of-disks state crystals differ significantly from the theoretical cold fluid result known to describe stationary, closed-shell structures well. By evoking the assumption that the string-of-disks states are rotating about the trap axis at an angular frequency $\sim \omega_{rf}/4$ we are able to reestablish agreement between theory and experiment.

This work was supported by the Danish Natural Science Research Council, by the Carlsberg Foundation, and by the Danish National Research Foundation through Aarhus Center of Atomic Physics (ACAP) and

QUANTOP—Danish National Research Center for Quantum Optics. We acknowledge valuable contributions by Kristian Mølhave during the construction of the experimental setup.

*Present address: Department of Physics, University of Otago, Dunedin, New Zealand.

Electronic address: nk@physics.otago.ac.nz

†Electronic addresses: drewsen@phys.au.dk

www.phys.au.dk/iontrapgroup

- [1] F. Diedrich, E. Peik, J. M. Chen, W. Quint, and H. Walther, *Phys. Rev. Lett.* **59**, 2931 (1987).
- [2] D. J. Wineland, J. C. Bergquist, W. M. Itano, J. J. Bollinger, and C. H. Manney, *Phys. Rev. Lett.* **59**, 2935 (1987).
- [3] W. M. Itano, J. J. Bollinger, J. N. Tan, B. Jelenković, X.-P. Huang, and D. J. Wineland, *Science* **279**, 686 (1998).
- [4] M. Drewsen, C. Brodersen, L. Hornekær, J. S. Hangst, and J. P. Schiffer, *Phys. Rev. Lett.* **81**, 2878 (1998).
- [5] H. C. Nägerl, W. Bechter, J. Eschner, F. Schmidt-Kaler, and R. Blatt, *Appl. Phys. B* **66**, 603 (1998).
- [6] T. B. Mitchell, J. J. Bollinger, X.-P. Huang, W. M. Itano, and D. H. E. Dubin, *Phys. Plasmas* **6**, 1751 (1999).
- [7] M. Block, A. Drakoudis, H. Leuthner, P. Seibert, and G. Werth, *J. Phys. B* **33**, L375 (2000).
- [8] D. H. E. Dubin and T. M. O'Neil, *Rev. Mod. Phys.* **71**, 87 (1999).
- [9] L. Hornekær, N. Kjærgaard, A. M. Thommesen, and M. Drewsen, *Phys. Rev. Lett.* **86**, 1994 (2001).
- [10] M. Drewsen, I. S. Jensen, N. Kjærgaard, J. Lindballe, A. Mortensen, K. Mølhave, and D. Voigt, *J. Phys. B* **36**, 525 (2003).
- [11] N. Kjærgaard, K. Mølhave, and M. Drewsen, *Phys. Rev. E* **66**, 015401 (2002).
- [12] E. D. Courant and H. S. Snyder, *Ann. Phys. (N.Y.)* **3**, 1 (1958).
- [13] N. Kjærgaard and M. Drewsen, *Phys. Plasmas* **8**, 1371 (2001).
- [14] N. Kjærgaard, L. Hornekær, A. M. Thommesen, Z. Vide-sen, and M. Drewsen, *Appl. Phys. B* **71**, 207 (2000).
- [15] See EPAPS Document No. E-PRLTAO-91-032332 for a video sequence showing the structural transition. A direct link to this document may be found in the on-line article's HTML reference section. The document may also be reached via the EPAPS homepage (<http://www.aip.org/pubservs/epaps.html>) or from <ftp.aip.org> in the directory /epaps/. See the EPAPS homepage for more information.
- [16] D. H. E. Dubin, *Phys. Rev. E* **53**, 5268 (1996).
- [17] R. W. Hasse and J. P. Schiffer, *Ann. Phys. (N.Y.)* **203**, 419 (1990).
- [18] R. W. Hasse and V. V. Avilov, *Phys. Rev. A* **44**, 4506 (1991).
- [19] D. H. E. Dubin and T. M. O'Neil, *Phys. Rev. Lett.* **60**, 511 (1988).